Journal of Power Sources 195 (2010) 165–169

Contents lists available at ScienceDirect

Journal of Power Sources

journal homepage: www.elsevier.com/locate/jpowsour

Short communication

A preliminary study of the electro-oxidation of L-ascorbic acid on polycrystalline silver in alkaline solution

L. Majari Kasmaee, F. Gobal*

Department of Chemistry, Sharif University of Technology, P.O. Box 11365-9516, Tehran, Iran

ARTICLE INFO

Article history:
Received 29 May 2009
Received in revised form 29 June 2009
Accepted 30 June 2009
Available online 7 July 2009

Keywords:
Silver
Ascorbate electro-oxidation
Electro-catalyst
Direct ascorbic acid fuel cell

ABSTRACT

Electrochemical oxidation of L-ascorbic acid on polycrystalline silver in alkaline aqueous solutions is studied by cyclic voltammetry (CV), chronoamperometry (CA) and impedance spectroscopy (IS). The anodic electro-oxidation starts at −500 mV versus SCE and shows continued anodic oxidation in the cathodic half cycle in the CV regime signifying slowly oxidizing adsorbates. Diffusion coefficient of ascorbate ion measured under both voltammetric regimes is around 1.4×10^{-5} cm^2 s^{-1}. Impedance spectroscopy measures the capacitances associated with double layer and adsorption around 50 μF cm^{-2} and 4 mF cm^{-2} as well as the adsorption and decomposition resistances (rates).

1. Introduction

Direct L-ascorbic acid fuel cells (DAAFCs) were introduced by Fujiwara et al. [1] to overcome a number of limitations of direct methanol fuel cells (DMFCs), namely, the large overvoltage toward the electro-oxidation of methanol [2], large methanol crossover through the polymer membrane [3] and the toxicity of methanol and its products, formaldehyde and formic acid, formed in the course of fuel cell operation.

L-Ascorbic acid, well known as vitamin C, offers some interesting characteristics as a fuel. It is environmentally and biologically friendly and can be obtained by the fermentation or chemical conversion of D-glucose [1]. L-Ascorbic acid is a famous reducing agent and its oxidation does not release any toxic product. In addition, it is proven that a membrane crossover phenomenon is not a problem in DAAFCs [4].

Some efforts have been done in order to introduce new anodes for DAAFCs, including, platinum group metals (PGMs) [4,5], Au [5] and carbon [5–7]. However due to the high cost of PGMs, discovery of a new metallic anode for DAAFCs is necessary. The purpose of this study is to investigate the activity of silver as anode material for L-ascorbic acid electro-oxidation. Due to the anodic dissolution of silver in acidic media, all the experiments were carried out in alkaline solutions. Cyclic voltammetry, chronoamperometry and electrochemical impedance spectroscopy were employed in this study. Electrocatalytic activity of silver was compared with the previously studied metallic anodes of DAAFCs [4,5].

2. Experimental

L-Ascorbic acid and sodium hydroxide used in this study were analytical grade of Merck origin and used without further purification. All solutions were prepared by distillated water and were purged with N_2 prior to experiments to prevent L-ascorbic acid oxidation by ambient oxygen. Electrochemical techniques including cyclic voltammetry, chronoamperometry, and electrochemical impedance spectroscopy were employed. All the electrochemical studies were performed in a conventional three-electrode cell powered by Voltalab model PGZ100 potentiostat/galvanostat. The system was run by a PC through VoltaMaster 4 and Zplot/Zview commercial software. The frequency range of 100 KHz to 1.5 Hz and the modulation amplitude of 10 mV were employed for impedance studies. A saturated calomel electrode (SCE) and a Pt foil were used as the reference and counter electrodes, respectively. Silver foil with the purity of 99.9% having geometric area of 15 mm^2 was used as the working electrode. Silver surface was cleaned with 2-propanol in order to remove oil and dirt and then rinsed with distillated water.

3. Results and discussion

3.1. Cyclic voltammetry

Typical cyclic voltammogram of silver in 1 M NaOH solution, in the potential range of −1800 to 900 mV versus SCE is shown

* Corresponding author. Tel.: +98 21 6600 5718; fax: +98 21 6601 2983.
E-mail address: gobal@sharif.ir (F. Gobal).

0378-7753/$ – see front matter © 2009 Elsevier B.V. All rights reserved.
doi:10.1016/j.jpowsour.2009.06.095

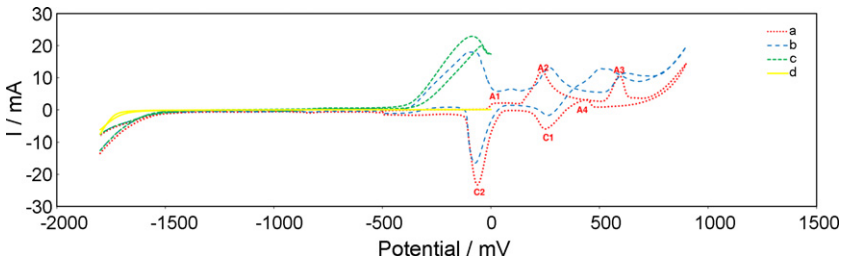

Fig. 1. Cyclic voltammograms on silver electrode in potential range of (a) −1800 to 900 mV, in 1 M NaOH, (b) −1800 to 900 mV, in 1 M NaOH + 0.25 M L-ascorbic acid, (c) −1800 to 0 mV, in 1 M NaOH + 0.25 M L-ascorbic acid, (d) −1800 to 0 mV, in NaOH solutions. Potential scan rate is 100 mV s^{-1}.

in Fig. 1a, where potential sweep rate of 100 mV s^{-1} has been employed. This voltammogram is in good agreement with those reported in the literature [8]. Comparing with the literature, a number of well defined anodic and cathodic peaks can be identified. The first small anodic peak (A1) is related to the electrodissolution of Ag to $[Ag(OH)_2]^-$ through adsorption of OH^- and desorption and diffusion of soluble $[Ag(OH)_2]^-$. The anodic peak A2 can be ascribed to the electroformation of multilayer of Ag_2O. This process has been reported to occur according to:

$$2Ag + 2OH^- \leftrightarrow Ag_2O + H_2O + 2e^- \quad (1)$$

The anodic peak A3 is due to the electro-oxidation of Ag_2O and the formation of AgO according to the overall chemical reaction:

$$Ag_2O + 2OH^- \leftrightarrow 2AgO + H_2O + 2e^- \quad (2)$$

The direct electro-oxidation of Ag to AgO may also occur [8] within the potential range of peak A3:

$$Ag + 2OH^- \leftrightarrow AgO + H_2O + 2e^- \quad (3)$$

The existence of anodic peak A4 at the reverse scan in the potential range of peak A2 could be attributed to continuous nucleation and growth of Ag_2O film as a result of direct electro-oxidation of Ag metal. The cathodic peak C1 is due to the electroreduction of AgO to Ag_2O, indicating that the peak is conjugated to the peak A3. The more negative cathodic peak C2 could be related to the processes involved in the electro-reduction of Ag_2O to Ag [8]. Previous studies [8] also show that if the potential is reversed before any oxidation peak appears, the reverse potential scan retraces itself and does not display any cathodic peak, which is confirmed experimentally (Fig. 1d), indicating that the anode surface is free of any passive layers. This key point assures us that ascorbate is electro-oxidized on pure silver surface and not on any of its oxides.

Cyclic voltammogram of silver electrode in 1 M NaOH solution containing 0.25 M L-ascorbic acid in the potential range of −1800 to 900 mV versus SCE is presented in Fig. 1b. The same expected pattern of silver redox processes are accompanied by a new large peak at −94 mV versus SCE which is due to ascorbate electro-oxidation. Fig. 1c presents the voltammogram where the anodic half cycle is terminated at 0 mV versus SCE. The same large anodic peak due to the oxidation of ascorbate ions appears at −90 mV versus SCE while in the cathodic half cycle a large anodic peak which is due to the slowly oxidized surface residues is observed at −60 mV versus SCE. The pattern is the well known behavior observed in the course of the electro-oxidation of many organics [9] on a variety of surfaces. No reduction peak has been observed in reverse potential scan, indicating the irreversible nature of ascorbate electro-oxidation on silver electrode.

The onset potential of ascorbate electro-oxidation on silver anode is −500 mV versus SCE which is significantly negative in comparison to those reported in the literature for other metals. For instance, it is reported that on Pt, Ru, Rh, Ir, Pd, PtRu, Au and also glassy carbon electrodes in acidic media, anodic current starts to increase around 500 mV versus RHE [5] which is nearly 700 mV higher than that observed in the present work. Also, the anodic peak current density of ascorbate electro-oxidation obtained in this study is considerably larger than anodic current density of the same process on other electrodes at the same L-ascorbic acid concentrations previously reported in the literature [5], confirming superior electrocatalytic activity of silver metal toward ascorbate electro-oxidation.

Fig. 2 presents cyclic voltammograms of silver electrode, recorded in 1 M NaOH solutions containing different concentrations of L-ascorbic acid, while the variation of peak current with concentration is presented in Fig. 3a. A very good linear dependency below 0.065 M has been witnessed. Fig. 3b presents the variation of anodic peak current against potential sweep rate. Fairly good linear dependency below 150 mV s^{-1} sweep rates and at the concentrations below 0.065 M has been observed. Diffusion coefficient of ascorbate is calculated through Randles–Sevcik equation [10]:

$$i_p = (2.69 \times 10^5) n^{3/2} A D^{1/2} C^* \nu^{1/2} \quad (4)$$

where i_p is the anodic peak current (A), ν is the scan rate (V s^{-1}), n is the number of electrons produced in oxidation process, A is the electrode geometric area (cm^2), D is the diffusion coefficient (cm^2 s^{-1}) and C^* is the bulk concentration of electroactive species (mol cm^{-3}). Similar ranges of potential sweep rates and concentrations as those of this work have been used in the literature [11–14] in conjunction with Eq. (4) for derivation of diffusion coefficients. On this basis the diffusion coefficient of ascorbate ion was found to be 1.4×10^{-5} cm^2 s^{-1}.

3.2. Chronoamperometry study

Two step chronoamperometry technique has been employed for the investigation of L-ascorbic acid oxidation process. The chronoamperograms of silver electrode in the absence (Fig. 4A(a)) and presence of various concentrations of L-ascorbic acid (Fig. 4A(b–e)) in 1 M NaOH at the oxidation potential step of −100 mV versus SCE and reduction potential step of −900 mV versus SCE, are presented in Fig. 4A. No current has been observed in the absence of L-ascorbic acid and in the presence of ascorbate the

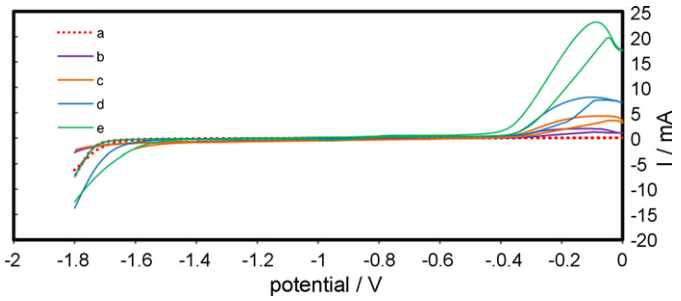

Fig. 2. Cyclic voltammograms on silver electrode in potential range of −1800 to 0, in 1 M NaOH solutions containing (a) 0 M, (b) 0.015 M, (c) 0.035 M, (d) 0.065 M, (e) 0.25 M L-ascorbic acid. Potential scan rate is 100 mV s^{-1}.

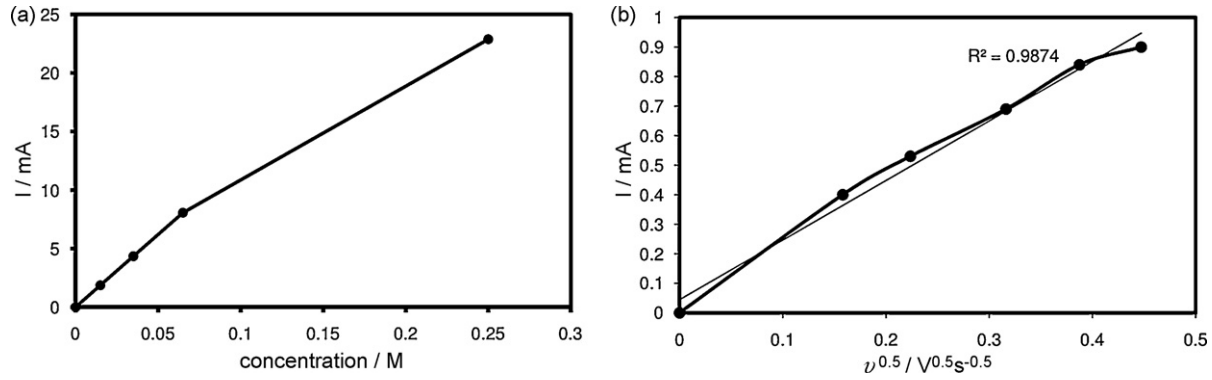

Fig. 3. (a) Dependency of the anodic peak current density on L-ascorbic acid concentration (from Fig. 2). (b) Dependency of the anodic peak current density on square root of potential scan rate. L-Ascorbic acid concentration is 0.01 M.

entire net current is thus due to the oxidation of this entity. The plot of net current versus $t^{-0.5}$ at 0.15 M L-ascorbic acid solution gives a straight line (Fig. 4B) which means that Cottrell equation (Eq. (5)) is obeyed in concentrations under 0.15 M of L-ascorbic acid and that the transient current is controlled by diffusion [9]:

$$i_t = \frac{nFAD^{1/2}C^*}{\pi^{1/2}t^{1/2}} \quad (5)$$

Here, i_t is the transient current (A), n is the number of electrons produced during oxidation process, F is Faraday constant (C mol^{-1}), A is the electrode geometric area (cm^2), D is the diffusion coefficient (cm^2 s^{-1}), C^* is the bulk concentrate on of electroactive species (mol cm^{-3}) and t is time (s). The concentration range used in this work (<0.15 M) is similar to those reported in the literature in such measurements [11–14]. The value of diffusion coefficient derived in this method was 1.42×10^{-5} cm^2 s^{-1} and in good agreement with our CV results. No significant cathodic current is observed when the electrolysis potential is stepped to −900 V versus SCE indicating the irreversible nature of the oxidation of ascorbate. The stability of the system was monitored by running the chronoamperometry for more extended periods of time where highly stable constant currents with no signs of instability, oscillation, etc. were observed (Fig. 5).

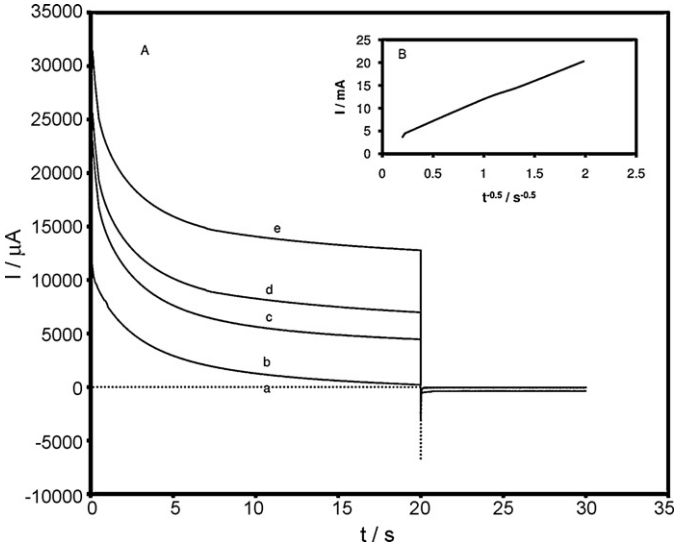

Fig. 4. (A) Double steps chronoamperograms of silver electrode in 1 M NaOH solution containing L-ascorbic acid with different concentrations of 0 M (a), 0.1 M (b), 0.15 M (c), 0.25 M (d), 0.5 M (e), respectively. Potential steps were −300 mV for oxidation and −900 mV for reduction. (B) Plot of net current of chronoamperogram of silver electrode in 0.15 M L-ascorbic acid versus $t^{-0.5}$.

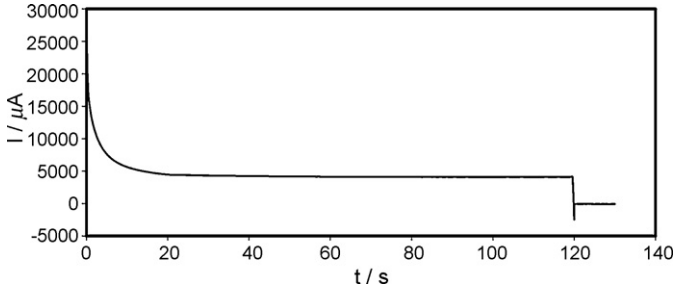

Fig. 5. Double steps chronoamperogram of silver electrode in 1 M NaOH + 0.15 M L-ascorbic acid recorded for 2 min. Potential steps were −300 mV for oxidation and −900 mV for reduction.

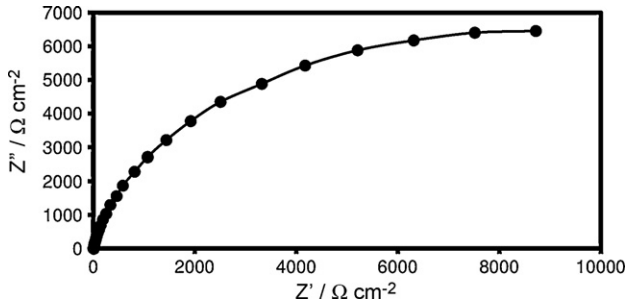

Fig. 6. Nyquist diagram of silver electrode in the 1 M NaOH solution. d.c.—potential is −300 mV versus SCE.

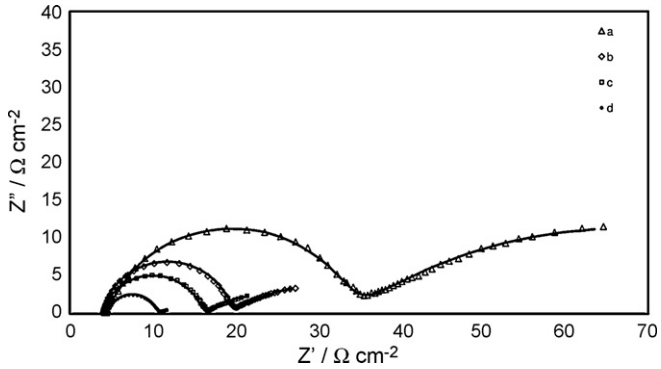

Fig. 7. Nyquist diagrams of silver electrode in (a) 0.05, (b) 0.15, (c) 0.25, (d) 0.5 L-ascorbic acid and 1 M NaOH solutions and the corresponding fitted curves. d.c. potential is −300 mV versus SCE.

Table 1
Fit values of the electrical elements in the electrical equivalent circuit presented in Fig. 8 obtained by fitting the complex-plane plots demonstrated in Fig. 6 and the corresponding relative errors.

R_s (Ω^{-1})	R_{ads} (Ω^{-1})	Q_{dl}		R_{ct} (Ω^{-1})	Q_{ads}		C_m (M^{-1})
		A ($\times 10^5\ \Omega^{-1}\ s^{\alpha}$)	α		A' ($\times 10^3\ \Omega^{-1}\ s^{\alpha'}$)	α'	
8.243 (1.67%)	–	0.40 (2.44%)	0.90 (0.48%)	15313.00 (0.87%)	–	–	0
4.080 (1.25%)	28.90 (1.27%)	8.21 (0.38%)	0.87 (1.20%)	73.89 (0.71%)	7.04 (3.81%)	0.76 (0.82%)	0.05
4.024 (0.22%)	15.09 (0.37%)	5.50 (0.48%)	0.95 (0.41%)	21.15 (1.40%)	3.48 (2.21%)	0.76 (0.65%)	0.15
4.018 (0.51%)	11.59 (0.61%)	4.92 (0.80%)	0.93 (0.73%)	19.28 (0.41%)	2.61 (1.24%)	0.75 (0.31%)	0.25
4.502 (0.53%)	5.890 (1.75%)	4.81 (1.05%)	0.94 (1.20%)	2.10 (1.91%)	1.95 (1.17%)	0.76 (0.88%)	0.50

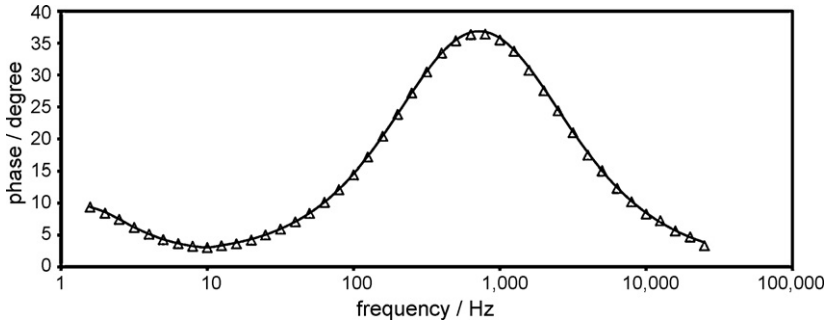

Fig. 8. Bode plot of silver electrode in 1 M NaOH and 0.15 M L-ascorbic acid. d.c. potential is −300 mV versus SCE. Symbols are experimental data and continuous line is fitted data.

3.3. Electrochemical impedance measurements

Fig. 6 presents the Nyquist plot of silver electrode recorded at −300 mV versus SCE d.c. offset potential, in 1 M NaOH solution. A slightly depressed semicircle signifying double layer capacitor charging which slightly leaks has been observed. The quantitative results are presented in Table 1 and are in agreement with the expectations [15].

The Nyquist diagrams of silver electrode recorded at −300 mV versus SCE d.c. offset, at various concentrations of L-ascorbic acid in 1 M NaOH solutions, are shown in Fig. 7. These consist of two slightly depressed semicircles at high and low frequency domains. The presence of two semicircles in the Nyquist diagrams are confirmed by Bode presentation, Fig. 8, which has also been recorded at −300 mV versus SCE and corresponds to the Nyquist plot presented in Fig. 7b. In this Bode plot, two peaks at 10^3 and 1.5 Hz frequencies signifying two time constants are observed.

Fig. 9 presents the equivalent circuit compatible with impedance results. While R_s is the electrolyte resistance, the semicircle in the low frequency end of the spectrum is associated with the formation and decomposition of adsorbed layer (charging of Q_{ads} through the resistance R_{ads} and its discharge via the resistance R_{ct}). The semicircle in high frequency side of the spectrum is associated with interfacial double layer charging and its leak through resistance R_{ads} for charging the adsorption capacitor and its subsequent

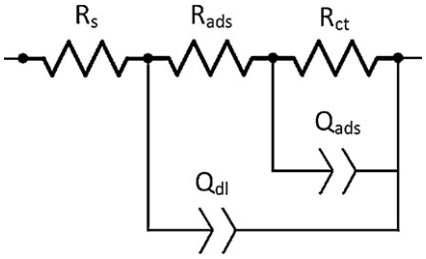

Fig. 9. The equivalent circuit that is used to simulate the electrode processes.

leakage through R_{ct}. In the equivalent circuit, ideal capacitors had to be replaced by constant phase elements (CPEs) to account for the experimentally observed squashed semicircles [15]. Table 1 presents the results of derivation of equivalent circuit elements based on a non-linear least square fit at various concentrations of L-ascorbic acid. Values around 50 μF cm^{-2} for double layer and 4 mF cm^{-2} for adsorption capacitances have been found.

The frequency dependence of total impedance can be represented by Eq. (6):

$$Z(j\omega) = R_s + \frac{R_{ct} + R_{ads}[1 + A'(j\omega)^{\alpha'} R_{ct}]}{[1 + A(j\omega)^{\alpha} R_{ads}] \times [1 + A'(j\omega)^{\alpha'} R_{ct}] + A(j\omega)^{\alpha} R_{ct}} \quad (6)$$

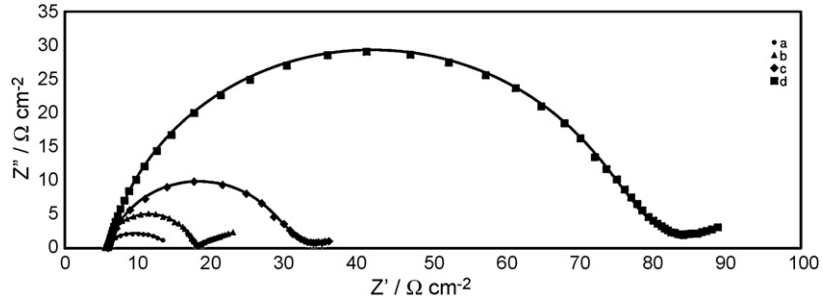

Fig. 10. Nyquist diagrams of silver electrode in 0.25 M L-ascorbic acid and 1 M NaOH solution recorded at (a) −100 mV, (b) −300 mV, (c) −350 mV, (d) −390 mV d.c. potentials versus SCE, and the corresponding fitted curves.

Table 2
Fit values of the electrical elements in the electrical equivalent circuit presented in Fig. 8 obtained by fitting the complex-plane plots demonstrated in Fig. 9 and the corresponding relative errors.

R_s (Ω^{-1})	R_{ads} (Ω^{-1})	Q_{dl}		R_{ct} (Ω^{-1})	Q_{ads}		$V_{d.c.}$ (mV)
		A ($\times 10^5\ \Omega^{-1}\ s^{\alpha}$)	α		A' ($\times 10^3\ \Omega^{-1}\ s^{\alpha'}$)	α'	
5.844 (0.71%)	69.72 (0.67%)	5.14 (0.69%)	0.88 (0.66%)	30.02 (3.47%)	4.38 (5.30%)	0.83 (0.96%)	−390
5.860 (1.38%)	23.44 (1.79%)	4.94 (2.69%)	0.85 (2.02%)	20.81 (3.04%)	2.86 (2.20%)	0.71 0.33%)	−350
4.018 (0.51%)	11.59 (0.61%)	4.42 (2.80%)	0.93 (0.73%)	19.28 (0.41%)	2.13 (4.24%)	0.75 (0.31%)	−300
6.095 (1.49%)	5.07 (1.13%)	3.82 (3.30%)	0.94 (0.30%)	6.64 (3.14%)	1.63 (4.17%)	0.70 (1.52%)	−100

where A and α are related to double layer while A' and α' are adsorption CPE parameters. ω is the frequency and other symbols have their usual and mentioned meanings. Fig. 10 presents the Nyquist plots recorded at different d.c. offset potentials at the L-ascorbic acid concentration of 0.25 M. Very good fits based on the proposed equivalent circuit (or Eq. (6)) have been achieved. The results of derivation of circuit elements are presented in Table 2. Perfectly justifiable trends as well as good consistencies between the values in Tables 1 and 2 have been witnessed. Both R's decrease upon increasing the anodic potential and reflect the speeding up of both adsorption and oxidative removal of the adsorbed species. Although the inverse of the R's values reflect the rates of the corresponding processes the derivation of the rates constants requires detailed knowledge of the mechanism and has not been attempted at this stage of this study. Adsorption rate seems to be more influenced by the applied potential, Table 2, and exceeds the rate of the removal of adsorbed species as the potential is made more anodic. The findings are in agreement with the pattern observed in cyclic voltammograms (Fig. 2).

4. Conclusions

On the basis of this work it is concluded that: (i) polycrystalline silver is a good electro-catalyst for the anodic oxidation of ascorbate ion with the oxidation onset around −500 mV versus SCE, (ii) the oxidation goes through the formation and decomposition of adsorbed intermediates and (iii) impedance spectroscopy was capable of providing the values of double layer and adsorption capacitances as well as resolving adsorption and decomposition resistances (rates).

Acknowledgment

The authors wish to express thanks to the office of vice chancellor of research of Sharif University of Technology for the financial support.

References

[1] N. Fujiwara, K. Yasuda, T. Ioroi, Z. Siroma, Y. Miyazaki, T. Kobayashi, Electrochem. Solid-State Lett. 6 (12) (2003) A257–A259.
[2] H. Liu, C. Song, L. Zhang, J. Zhang, H. Wang, D.P. Wilkinson, J. Power Sources 155 (2) (2006) 95–110.
[3] A. Heinzel, V.M. Barragan, J. Power Sources 84 (1) (1999) 70–74.
[4] N. Fujiwara, S. Yamazaki, Z. Siroma, T. Ioroi, K. Yasuda, J. Power Sources 167 (1) (2007) 32–38.
[5] N. Fujiwara, Z. Siroma, T. Ioroi, K. Yasuda, J. Power Sources 164 (2) (2007) 457–463.
[6] S. Uhm, J. Choi, S.T. Chung, J. Lee, Electrochim. Acta 53 (4) (2007) 1731–1736.
[7] N. Fujiwara, S. Yamazaki, Z. Siroma, T. Ioroi, K. Yasuda, Electrochem. Commun. 8 (5) (2006) 720–724.
[8] S.S.A. El Rehim, H.H. Hassan, M.A.M. Ibrahim, Monatsh. Chem. 129 (11) (1998) 1103–1117.
[9] Southampton Electrochemistry Group, Instrumental Methods in Electrochemistry, University of Southampton, Ellis Horwood, Chichester, 1990.
[10] J.E.B. Randles, Trans. Faraday Soc. 44 (1948) 327–338.
[11] L. Zheng, J. Song, J. Solid State Electrochem. (2009), doi:10.1007/s10008-008-0780-3.
[12] R. Ojani, J. Raoof, S. Fathi, Electrochim. Acta 54 (2009) 2190–2196.
[13] H. Heli, M. Jafarian, M.G. Mahjani, F. Gobal, Electrochim. Acta 49 (2004) 4999–5006.
[14] M. Jafarian, M.G. Mahjani, H. Heli, F. Gobal, H. Khajehsharifi, M.H. Hamedi, Electrochim. Acta 48 (2003) 3423–3429.
[15] E. Barsoukov, J.R. Macdonald, Impedance Spectroscopy: Theory, Experiment, and Applications, second ed., Wiley, New York, 2005.